Nuclear Instruments and Methods in Physics Research B 319 (2014) 146–153

Contents lists available at ScienceDirect

Nuclear Instruments and Methods in Physics Research B

journal homepage: www.elsevier.com/locate/nimb

# Bulk observation of aluminum green compacts by way of X-ray tomography

Shidi Yang [a], Wei Fang [b], Yongheng Chi [a], Dil Faraz Khan [b,c], Ruijie Zhang [b], Xuanhui Qu [a,b,*]

[a] State Key Laboratory for Advanced Metals and Materials, University of Science and Technology Beijing, Beijing 100083, People's Republic of China
[b] School of Material Science and Engineering, University of Science and Technology Beijing, Beijing 100083, People's Republic of China
[c] Department of Physics, University of Science and Technology Bannu, Bannu 28100, Pakistan

ARTICLE INFO

*Article history:*
Received 5 July 2013
Received in revised form 8 September 2013
Available online 3 December 2013

*Keywords:*
Green compact
Relative density distribution
Pore
Image processing

ABSTRACT

A quantitative X-ray tomographic analysis of the relative density distribution and porosity in green compacts is presented. In this study, image processing is used to quantify binary images obtained from original reconstructed images. After 3D reconstruction using the binary images, quantitative observations from the 3D renderings are performed to analyze the relative density distribution of the green compacts. On the basis of the results, the different relative density distributions of the green compacts pressed by different pressures are discussed. Statistical morphological analysis of the pores in the green compacts is also performed and the results confirm that the morphological characteristics of the pores are different in the case of different compaction pressures.



## 1. Introduction

Compaction is a molding treatment that uses pressure to transform loose metallic or ceramic powders into bulk green compacts containing residual pores. It is an important manufacturing technique used in mass production of semi-manufactured goods (often used for subsequent sintering) and final products. The most important parameter of compaction is the relative density of green compact. This parameter not only serves as a measurement of the quality of the compaction process but also determines the behavior of the green compacts during sintering.

Stress distribution in green compacts is complex; therefore, it cannot be obtained simply by dividing the compaction load by the cross-section area. Thus, the various relative density distributions and porosities may appear during direct die compaction [1]. Although this problem has been modeled [2,3] using numerical simulations and predicted by many empirical formulas such as Hackel equation [4,5], the distribution cannot be accurately described for all situations and the calculated results also can not be verified by the actual test results accurately. Briscore has used sectioning techniques to resolve these problems [6]. However, the method is time consuming and its precision cannot be guaranteed. Conventional observation approaches, such as scanning electron microscopy (SEM) and optical microscopy, have been used to observe the internal structure of many materials. However, these techniques require sample preparation techniques such as cutting and polishing that introduce artifacts into the samples and change the original internal structure [7].

X-ray tomography can be used for non-destructive qualitative and quantitative characterization of the microstructures and internal morphologies of materials [7–9]. The interior of the specimen can be thoroughly studied without resorting to physical or chemical treatment. Moreover, after scanning is complete, the samples can be reused for other tests [10].

Samples with small enough size can be analyzed at very high resolution (0.5–1.6 μm) by X-ray tomography [11–13], allowing detailed characterization of their internal microstructures. However, this method precludes direct comparison of the different parts of the bulk material, and may introduce artificial defects during sample preparation. Therefore, the aim of this paper is to show that bulk observation of aluminum powder green compacts with original size can be performed using X-ray tomography. This paper is divided into three main sections. The first section describes the image processing methods used to obtain binary images from original reconstructed images. Then, the 3D rendering of each green compact is reconstructed by the binary images. The second section describes the relative density distribution of each green compact, and discusses some problems that can't be explained by conventional compaction theory. In the third section, morphological analysis of pores in the different green compacts is presented.

* Corresponding author at: State Key Laboratory for Advanced Metals and Materials, University of Science and Technology Beijing, Beijing 100083, People's Republic of China. Tel./fax: +86 10 62334311.
*E-mail address:* quxh@ustb.edu.cn (X. Qu).

0168-583X/$ - see front matter © 2013 Elsevier B.V. All rights reserved.
http://dx.doi.org/10.1016/j.nimb.2013.10.010

## 2. Experiments and methods

### 2.1. Compaction and X-ray tomographic scan

Cylindrical aluminum green compacts ($\Phi$ = 10 mm, $m$ = 1.5 g) were obtained using compaction pressures of 300, 460, 620 MPa, denoted as GC1, GC2, GC3, respectively. The die wall is not lubricated. The granularity of the aluminum powder (producer: Beijing Gaoye Science and Technology Co. Ltd.) was 325 mesh. After compaction, X-ray tomographic scanning was performed on the green compacts. The X-ray tomographic equipment used in this study was supplied by National X-ray digital imaging instrument center, China and the model number is μCT 130–13. The X-ray tube acceleration voltage was set at 130 kV and the tube current was set at 200 μA. The samples were rotated through 360° with angular increments of 0.9°, and a scan image was taken at each position. After scanning, the CT datasets were used to produce a series of original reconstructed slice images by means of back projection algorithm. Samples were also observed by MV6000 optical microscope.

### 2.2. Image processing

#### 2.2.1. Denoising and image enhancement

In X-ray tomographic original reconstructed images, noise always exists. Thus, an adaptive median filter was employed to remove noise. Compared to the conventional median filter, the adaptive median filter is better at handling impulse noise and more details in image can be preserved because the size of the rectangular filter window changes during filter operation, allowing it to adapt to the actual conditions.

If there is insufficient difference in the gray values between the phases, errors may occur during conventional threshold segmentation [14]. To provide greater segmentation accuracy, wavelet transform and an 'unsharp' mask were applied to perform the image enhancement. This operation can significantly improve the contrast between phases and decrease the amount of blurring in the images.

Wavelet transform is a powerful tool for the decomposition of different scales of textures. An image can be broken down into one low frequency image and three high frequency images after wavelet transformation. The low frequency image can be decomposed into the next level of low frequency and high frequency images, as the wavelet transform continues. Fig. 1 shows a sketch map which has been transformed three times, where LH represents the high frequency details in the vertical direction, HL represents the high frequency details in the horizontal direction, and HH represents the high frequency details in the diagonal direction. Thus, the various details of the original image can be extracted using the decomposed images.

In this study, the images were transformed three times. Then, every high frequency image was enhanced using 'unsharp' mask. In this step, the contrast between various details in the original images can be significantly improved. As shown in Fig. 1, the original image can be reconstructed by using the high frequency images. Thus, after the reconstruction of the enhanced high frequency images, the original images were effectively enhanced. Fig. 2A shows the gray scale image after noise removal and image enhancement.

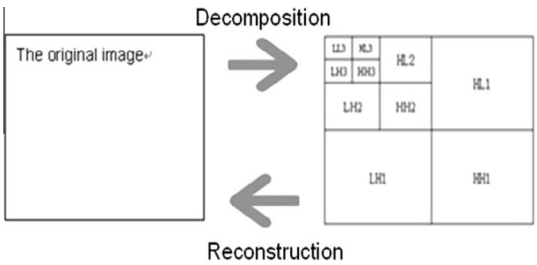


**Fig. 1.** Sketch image of 3-level wavelet transformation.

Because it is difficult to observe the changes of the reconstructed images after image processing visually, the effects of every image processing on a sample image is shown as follows. Fig. 3A is the original image and Fig. 3B is the image after being added noise. Fig. 4A and B are the results of noise removal operation by using median and adaptive median filter, respectively. From these two images, it can be seen that the noise is removed by the two filters very well. However, by comparing the two figures, especially the stamen in the images, the sharpness of Fig. 4B is higher than that of Fig. 4A. Thus, compared to the traditional median filter, more details in the original image are retained by the operation of adaptive median filter. The results of image enhancement are shown by Fig. 4C. By comparing the Fig. 4B and C, especially the leaf vein in the images, it can be seen that the contrast in the original image is greatly improved.

#### 2.2.2. Threshold segmentation

After previous image processing, an iteration method was employed for threshold value calculation. Gray values below the threshold value were assigned to pores and the ones larger than the threshold value were identified as aluminum powder particles. The procedures of iteration method are summarized as follows:

(a) Select an original value for the global threshold, $G$.
(b) Segment the image by using $G$. Two groups of pixels can be obtained: $G1$ consisting all pixels with intensity values greater than $G$, and $G2$ consisting of pixels with intensity values less than or equal to $G$.

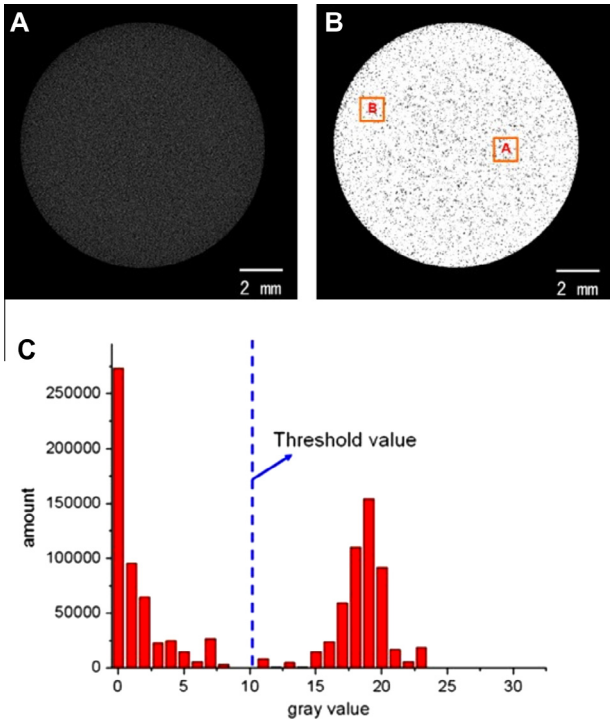


**Fig. 2.** (A) Gray scale image after noise removal and enhancement. (B) Binary image after image segmentation. (C) Gray histogram and the calculated threshold value of the corresponding gray scale image.